Received: 22 March 2022 | Revised: 20 September 2022 | Accepted: 17 October 2022

DOI: 10.1111/jbi.14534

Journal of Biogeography | WILEY

RESEARCH ARTICLE

Acoustic seascape partitioning through functional data analysis

Alejandro Ariza[1] | Anne Lebourges-Dhaussy[2] | David Nerini[3] | Etienne Pauthenet[4] | Gildas Roudaut[2] | Ramilla Assunção[5] | Everton Tosetto[5] | Arnaud Bertrand[1]

[1]MARBEC, Univ Montpellier, CNRS, Ifremer, IRD, Sète, France

[2]LEMAR, UBO, CNRS, IRD, Ifremer, Plouzané, France

[3]Mediterranean Institute of Oceanography, Aix-Marseille Université, CNRS/INSU, Université de Toulon, IRD, Marseille, France

[4]Sorbonne Universités, UPMC Université, Paris, France

[5]Laboratório de Oceanografia Física Estuarina e Costeira, Depto. Oceanografia, UFPE, Recife, Brazil

Correspondence
Alejandro Ariza, MARBEC, Univ Montpellier, CNRS, Ifremer, IRD, Sète, France.
Email: alejandro.ariza@ird.fr

Funding information
IRD Fellowship; International Joint Laboratory TAPIOCA; Horizon 2020, Grant/Award Number: 817578 and 73427

Handling Editor: Hudson Pinheiro

Abstract

Aim: Water column acoustic backscatter is regularly registered during oceanographic surveys, providing valuable information on the composition and distribution of pelagic life in the ocean. We propose an objective approach based on functional data analysis to classify these acoustic seascapes into biogeographical regions.

Location: Tropical South Atlantic Ocean off northeastern Brazil.

Taxon: Sound-scattering pelagic fauna detected with acoustic echosounders, principally small fish, crustaceans, squid and diverse gelatinous life-forms.

Methods: We use acoustic backscatter as a function of depth, simultaneously at three frequencies, to numerically describe the vertical distribution and composition of sound-scattering organisms in the water column. This information is used to classify the acoustic seascape through functional principal component analysis. The analysis routine is tested and illustrated with data collected at 38, 70 and 120 kHz in waters affected by contrasting environmental conditions.

Results: Acoustic seascape partitioning mirrored the distribution of current systems, fronts and taxonomically based regionalization. The study area was divided between slope-boundary and open-ocean waters, and between spring and fall hydrological regimes.

Main Conclusions: The acoustic seascape consistency and the spatiotemporal coherence of the regions classified show that the method is efficient at identifying homogeneous and cohesive sound-scattering communities. Comparisons against hydrological and biological regionalization prove that the method is reliable at delineating distinct pelagic ecosystems in a cost-efficient and non-intrusive way.

KEYWORDS
biogeography, echoregions, Fernando de Noronha, mesopelagic, micronekton, northeastern Brazil, sound-scattering layers, soundscape

1 | INTRODUCTION

Pelagic ecosystems are the largest living space in the ocean. It is a three-dimensional aquatic environment away from the seabed where small crustaceans, fish, squid and a variety of gelatinous life-forms make up the bulk of animal biomass (Murray & Hjort, 1912). Collectively, they can be referred as zooplankton or micronekton depending on their ability to swim against currents (Brodeur

et al., 2005). They are the link between primary production and top predators (Choy et al., 2016), but also between surface and the deep ocean by undertaking extensive vertical migrations that fuels the water column with organic matter (Ariza et al., 2015; Saba et al., 2021). Zooplankton and micronekton inhabit a vast three-dimensional space, influenced by different physical and biogeochemical regimes, such as light, temperature, oxygen or productivity (Aksnes et al., 2017; Bertrand et al., 2011; Boswell et al., 2020). Their distribution and composition change across eddies, fronts, internal waves and water masses, being affected by both local- and large-scale processes (Béhagle et al., 2016; Bertrand et al., 2014; Godø et al., 2012; Kaartvedt et al., 2012; Klevjer et al., 2016).

As a result of these complex spatial patterns, it is difficult to investigate the distribution of zooplankton and micronekton solely through traditional net sampling. Instead, this research is often complemented with continuous and higher-resolution observation instruments such as acoustic echosounders (Godø et al., 2014; Handegard et al., 2013). Water column backscatter is nowadays regularly recorded during oceanographic research surveys. When collected in mobile platforms, continuous series of these vertical profiles form acoustic seascapes, where the spatial distribution of sound-scattering organisms can be observed along the surveyed transect. While not all organisms are efficiently detected with echosounders (Dornan et al., 2019; Proud et al., 2019), acoustic seascapes are useful to study the structure and composition of pelagic ecosystems (Benoit-Bird & Lawson, 2016). In fact, along-track differences in the shape and scattering properties of profiles often reveal the presence of ocean fronts or ecosystem transitions (Escobar-Flores et al., 2020; Godø et al., 2012; Nero et al., 1990).

Historically, acoustic classification methods were aimed at identifying specific targets and not entire water-column profiles (Fernandes et al., 2005; Korneliussen et al., 2018). However, new promising approaches have emerged in recent years to extract temporal or spatial patterns, using acoustic profiles as the unit of classification. While some of these methods extracted distribution metrics (Urmy et al., 2012) or scattering layer features (Proud et al., 2015, 2018) to parametrize profiles, others used the profile signal itself (Lee & Staneva, 2020; Receveur et al., 2020). Ideally, a combination of aspects such as vertical distribution, magnitude and the frequency response of backscatter, all along the acoustic profile, would yield the most comprehensive seascape classification. This would be equivalent to taxonomically based marine regionalization where the spatial assemblage, the proportions and composition of communities are key aspects to delineate ecosystems (Longhurst, 2010; Spalding et al., 2007).

Functional data analysis (FDA) is a branch of statistics that operates with functions rather than discretized data vectors. It encompasses a set of tools similar to those in conventional statistics such as the analysis of variance or principal component analysis (PCA) but operating with functions instead of discrete values (Ramsay & Silverman, 2005). In this way, FDA can parametrize and analyse the shape of any signal varying over a physical continuum, typically, time or space. FDA has been long used in the fields of economics, medical sciences or meteorology, but also in oceanographic studies, exhibiting a great potential at classifying temperature and salinity profiles in the ocean (Assunção et al., 2020; Nerini et al., 2010; Pauthenet et al., 2017). With conventional statistics, the analysis of variance or PCA in a set of oceanographic profiles would yield the same result even if we permuted the order of values along the depth dimension. With FDA, on the contrary, results would be different because the method explicitly considers the along-depth distribution of values. This makes FDA specially suitable to describe and classify profiles according to their shape, a feature that has proven of great utility to delineate systems and fronts in the ocean (Assunção et al., 2020; Pauthenet et al., 2017).

Here we propose a novel approach based on FDA to describe and classify acoustic seascapes. The method do not rely on metrics or features extracted from acoustic profiles. Instead, we look at the shape of the signal along the depth dimension, considering the full information embedded in the profiles, simultaneously at 38, 70 and 120 kHz. This functional and multifrequency approach enables to explicitly consider the vertical assemblage of distinct biological components within the water column, allowing an effective visualization of how the system changes along the surveyed area. Similarly to the term 'ecoregion', referred in biogeography to areas with characteristic species assemblages (Longhurst, 2010; Spalding et al., 2007), here we introduce the term 'echoregion', referred to areas with particular assemblages of sound-scattering pelagic organisms.

The analysis routine is tested and illustrated on acoustic data collected in waters off northeastern Brazil, an area in the western Tropical Atlantic influenced by coastal processes, island mass effects and the convergence of major ocean currents systems (Assunção et al., 2020; Dossa et al., 2021). We describe the application of FDA on multifrequency echosounder data for the first time, and provide an open-source software to facilitate future implementations of the method. Additionally, we discuss the results in the context of oceanographic and ecological features of the studied area.

2 | MATERIALS AND METHODS

2.1 | Data collection

Two oceanographic surveys, ABRACOS I and ABRACOS II, were performed in the Southwest tropical Atlantic in Austral spring 2015 (September 29–October 21) and fall 2017 (April 9–March 8), as part of the project 'Acoustics along the Brazilian coast' (Bertrand, 2015, 2017). The sampling areas included the continental slope off northeastern Brazil, and oceanic waters around the islands and seamounts of the Fernando de Noronha Chain. Acoustic transects were conducted perpendicularly over the continental slope, and radially around the Rocas Atoll and the Fernando de Noronha Archipelago (Figure 1; Figure S1). Acoustic data were collected with a SIMRAD EK60 echosounder at 38, 70 and 120 kHz, synchronously transmitting every 2–3 s. Volume backscattering strength 'S_v' (dB re 1 m^{-1}; MacLennan et al., 2002) was

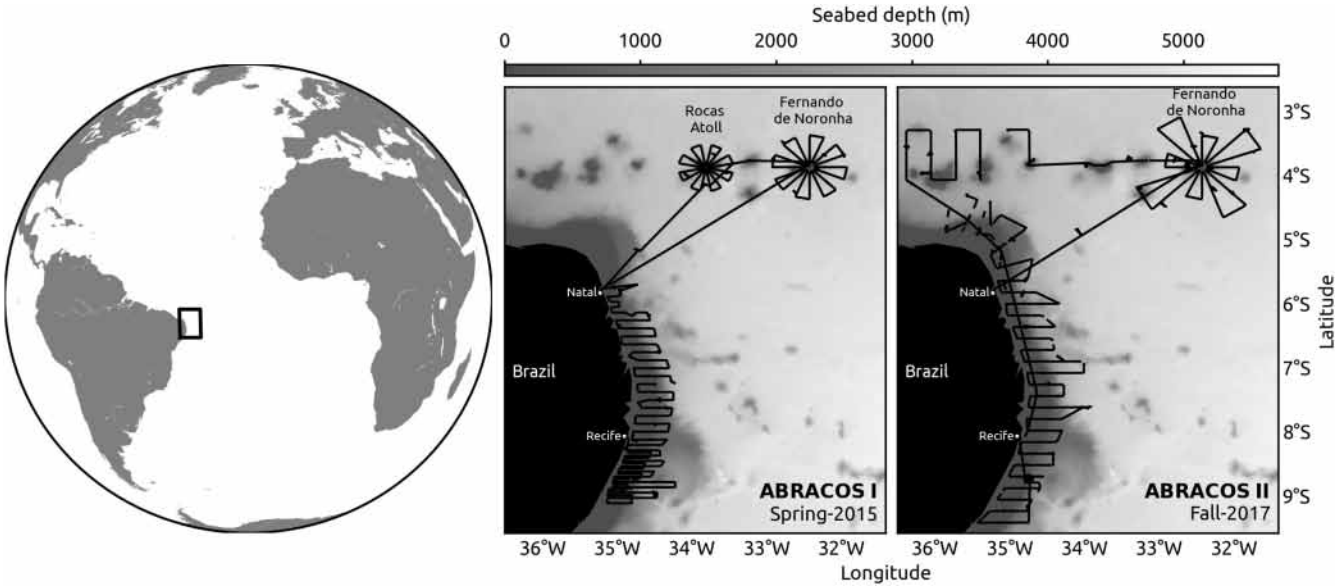

FIGURE 1 Sampling area and ship track (black line) for ABRACOS I and ABRACOS II surveys, conducted in Austral spring 2015 and fall 2017, respectively.

recorded down to 700 m depth with a pulse duration of 512 μs, beam angle of 7°, and a transmit power of 1000, 750 and 200 *W* at 38, 70 and 120 kHz, respectively. Standard target calibration of the echosounder was conducted prior to data acquisition (Demer et al., 2015).

2.2 | Data processing

Acoustic data were processed using the open-source library EchoPY v1.1, (2020), implemented in Python 3. Near-surface noise was avoided by excluding the signal from the transducer to a fixed distance of 10 m. Background noise was estimated and subtracted using the approach of De Robertis and Higginbottom (2007). Low signal-to-noise regions were excluded in two steps. First, samples with signal-to-noise ratios below 10 dB were set to −999 dB. Second, the depth range where background noise was above −80 dB was removed. Single-ping interferences from other instruments, and periods with either noise or attenuated signal due to inclement weather, were removed using the filters described by Ryan et al. (2015). S_v data were vertically and horizontally downsampled, by computing the arithmetic mean in the linear domain, to a resolution of 2 m by 2000 m, respectively. Such resolution was chosen to prevent ephemeral horizontal features to be considered, as the present study was aimed at analysing larger regional-scale patterns of the acoustic seascape. Only acoustic profiles collected at isobaths deeper than 1000 m were included in the analysis.

2.3 | Functional data analysis

Functional data analysis was used to simultaneously consider variations of the S_v signal at 38, 70 and 120 kHz, as a function of depth. This enabled to numerically describe and classify each acoustic profile according to the along-depth distribution of distinct sound-scattering organisms. This analysis was conducted separately on daytime and nighttime data, but mixing the two sampling periods, Spring 2015 and Fall 2017. Dawn and dusk time was excluded from the analysis by removing profiles where the centre of the sun was between 0° and 18° below the horizon, following the astronomical definition of twilight. A summary flowchart documenting the methodology sequence for the use of FDA is presented in Figure 2 and described below. All functions required to implement the FDA routine, as described in the present study, are publicly available within the analysis module of EchoPY v1.1 (2020).

2.3.1 | From discrete to functional data

First, discrete data from acoustic profiles must be converted into continuous curves using a decomposition in a basis system (Figure 2, step 1). Basis systems are linear combinations of known basis functions (ϕ_k) adjusted on the data, where the user can choose the type and number of functions or even apply constraints to tune the fitting process (Ramsay & Silverman, 2005). Here we chose a 'B-spline' basis, which is built upon spline functions, as the most suitable approximation system for non-periodic functional data (de Boor, 1978). The mathematical expression can be summarized as follows:

$$x_n^i(z) = \sum_{k=1}^{K} c_{n,k}^i \phi_k(z), i \in \{u38, u70, u120, m38, m70, l38\}, n = 1, \ldots, N, \quad (1)$$

where $c_{n,k}^i$ is the coefficient of decomposition for the basis function ϕ_k, which is dependent on the depth dimension z and is defined for a

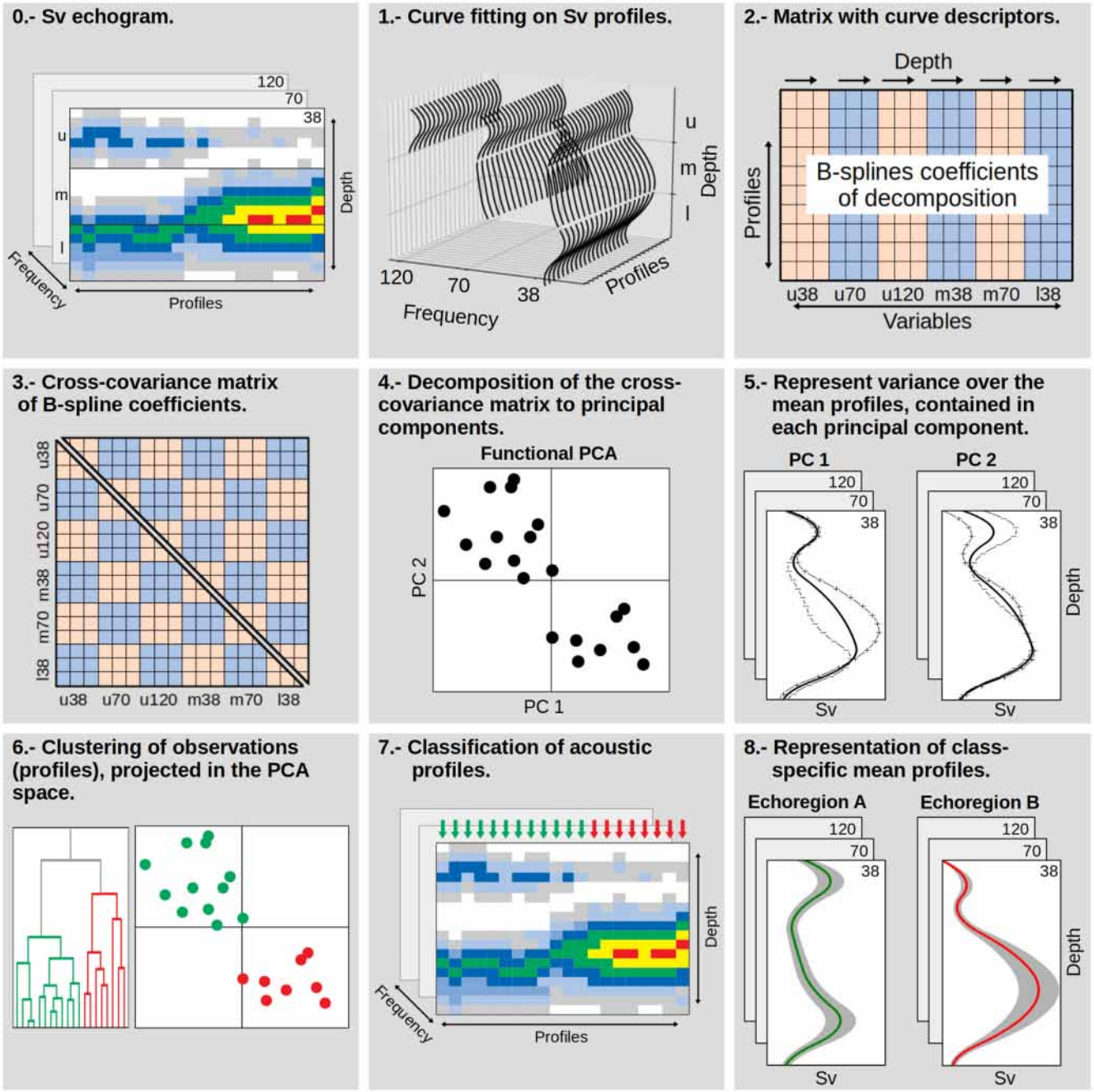

FIGURE 2 Implementation of the method. Acoustic data are segmented in upper (u), mid (m) and lower (l) depth intervals of equivalent range at 38, 70 and 120 kHz frequencies. For every profile, six curves are fitted, one for every depth-frequency segment where the acoustic signal is available: u38, u70, u120, m38, m70 and m120. Profiles and their curve descriptors are stored in a data matrix as rows and columns, respectively. The cross-covariance matrix is computed and decomposed into principal components (PCs) through functional principal component analysis (PCA). The variance induced in the water column by each PC and for any frequency can be explored and then a suitable number of these PCs are selected to classify the acoustic seascape. Each step of this figure is described in detail in Section 2.3.

given spatial location n and variable i. The number and the degree of basis functions (N) control the flexibility and the fitting performance of the basis system with respect to the actual data points. The more basis functions and the higher the degree, the better it will keep the vertical complexity of the original profile. On the contrary, few basis of low degree will be better to smooth out high-frequency variability in exchange to target broader vertical patterns in the water column. The number of basis is a user decision. It depends on the vertical variability that the study aims to represent and analyse. Here, regional-scale acoustic features were mainly sound-scattering layers with a vertical extent greater than 10 m. We found therefore appropriate to use a third-degree basis function every 10 m depth to represent the

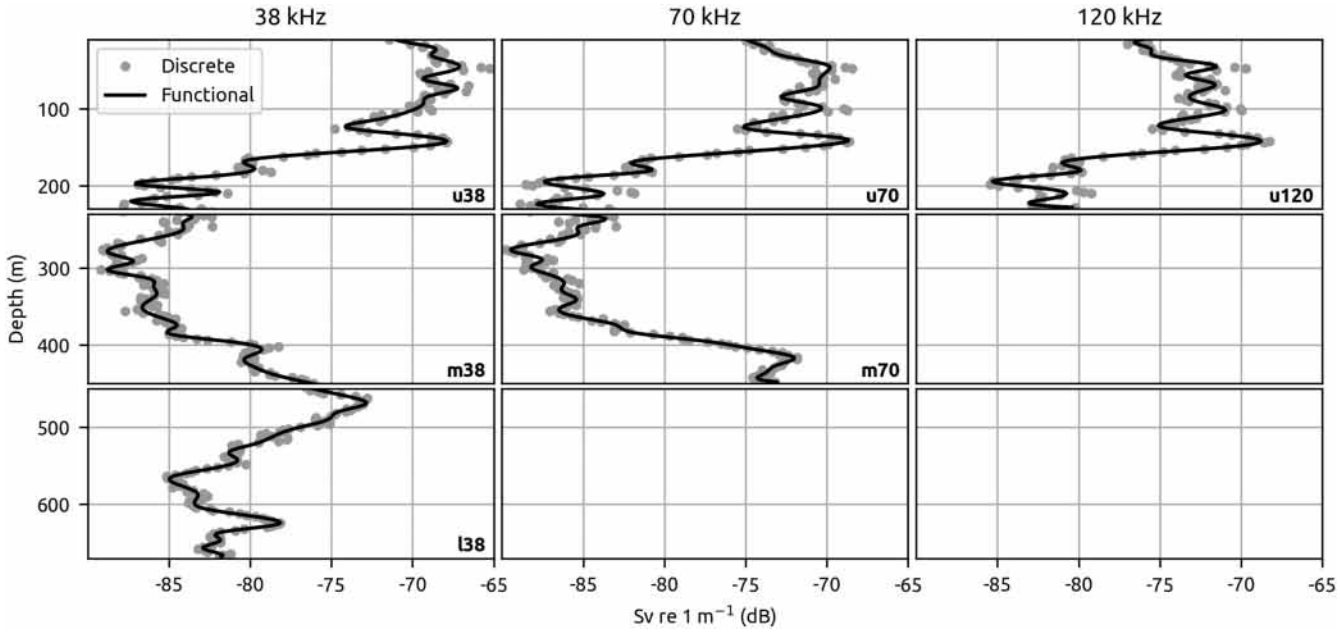

FIGURE 3 Functional data variables analysed: Upper 38, 70 and 120 kHz (u38, u70 and u120), mid 38 and 70 kHz (m38 and m70) and lower 38 kHz (l38). Upper, mid and lower refer to 220 m depth intervals with the following limits: 10–230, 230–450 and 450–670 m.

underlying vertical structure of the surveyed region without overfitting (Figure 3).

2.3.2 | Defining functional variables

A requirement for multivariate FDA is that all variables within the same observation need to be approximated with a consistent basis system. Which means that they must be built with the same type and number of basis functions, and use the same independent variable. The challenge with multifrequency acoustics is that the independent variable, depth, is not consistent. For this study, acoustic data were available from 10 m to approximately 700, 450 and 250 m depth, at 38, 70 and 120 kHz, respectively. Depending on the background noise conditions during the survey. If the same number of basis functions were adjusted to every frequency, we would end up with basis systems of inconsistent vertical resolution. To solve this issue, we broke up the three frequencies into six variables covering identical vertical extent along consecutive depth ranges (Figure 3). We defined the following variables for every observation: upper-38, upper-70, upper-120, mid-38, mid-70 and lower-38 (u38, u70, u120, m38, m70 and l38). Where 'upper', 'mid' and 'lower' refer to 220 m vertical intervals, from 10 to 230, 230 to 450 and 450 to 670 m depth, respectively (Equation 1; Figure 3). These six variables were then approximated with a B-spline basis system consisting in 22 third-degree polynomial basis, regularly distributed along 220 m. This resulted in a consistent resolution of 10 m per polynomial basis for the variables u38, u70, u120, m38, m70 and l38. After FDA, and to properly visualize results, the six variables were joined back into the three original frequency profiles.

2.3.3 | Functional PCA

To explore the along-depth S_v variance in the surveyed area, we applied functional principal component analysis (fPCA; Ramsay & Silverman, 2005) using the curve descriptors of the six variables presented in Section 2.3.2. In a discretized data scenario, a conventional PCA would be applied over a data matrix of n observations by m S_v values concatenated from 38, 70 and 120 kHz profiles. In a functional scenario, and for the application of a fPCA, the counterpart of the S_v values are the function coefficients, which in this case are those concatenated from the variables u38, u70, u120, m38, m70 and l38. This resulted in a data matrix with 1057 daytime or 1542 nighttime observations by 6×22 function coefficients (Figure 2, step 2). Each block of variables is then divided by its own variance as a normalization step usual in conventional PCA and a cross-covariance matrix is computed afterwards (Figure 2, step 3). The fPCA consists in finding the unique decomposition of the cross-covariance matrix that concentrate the variance explained by a minimum number of modes. These modes define a subspace in which each observation can be projected. The projections are the new variables called principal components (PCs) and the first ones represent the most significant modes of data variation (Figure 2, step 4). Once the fPCA has been solved, positive and negative perturbations on the averaged acoustic profiles can be examined by adding or subtracting the variance contained in each PC. This allowed to decouple the different modes of variation in the acoustic profiles, and quantify this variation at any given depth and frequency (Figure 2, step 5). Particularities on the fPCA computation, with respect to conventional PCA, can be found in Ramsay and Silverman (2005). All the operations performed in fPCA after the matrix of coefficients is obtained were implemented as in Pauthenet et al. (2017), and made publicly available in the open-source library associated to this study (FDA module in EchoPY v1.1, 2020).

2.4 | Clustering

Acoustic profiles were classified using 9 PCs, which contained 76% and 83% of the total variance of daytime and the nighttime datasets, respectively. We used agglomerative hierarchical clustering to evaluate the hierarchical structure of the classification (Figure 2, step 6). The 'Ward' linkage method was chosen as the most appropriate method to deal with globularly-distributed data (see Scikit-learn clustering module in Python). Groups of acoustic profiles with similar shape at 38, 70 and 120 kHz, as derived from hierarchical clustering, were referred here as 'classes'. If those classes exhibited spatiotemporal coherence (Figure 2, step 7) and consistent acoustic profiles (Figure 2, step 8), we referred to them as echoregions.

2.5 | Ancillary environmental and biological data

To discuss the distribution of echoregions in relation to environmental and biological features in the area, acoustic classification results were accompanied with ancillary data. Seabed was mapped at 15 arc seconds resolution from the GEBCO (2019) bathymetry. Thermohaline regions were extracted from Assunção et al. (2020). Current velocity fields were collected and processed as in Dossa et al. (2021) and horizontally resampled through linear interpolation to match the spatiotemporal resolution of the acoustic profiles. Biological regionalization was obtained from Eduardo et al. (2021), based on the horizontal assemblage of lanternfish species (Myctophidae) and from Tosetto et al. (2022), based on the distribution patterns of *Pyrosoma atlanticum* (Thaliacea). Additionally, the distribution patterns of physonect siphonophores (Hydrozoa) are included in the present study. Siphonophores were sampled through oblique hauls from 200 m depth to surface, using a Bongo net with a mouth diameter of 0.6 m and mesh size of 300 μm. The number of pyrosome and siphonophore colonies was standardized by water volume filtered at each haul. Siphonophores colonies were roughly estimated by dividing by 10 the number of nectophores found in each sample. Further information about biological sampling and processing can be found in Eduardo et al. (2021) and Tosetto et al. (2021, 2022). Thermohaline and current velocity fields, as well as lanternfish, pyrosomes and siphonophores distribution charts were obtained in parallel to the acoustic survey.

3 | RESULTS

3.1 | Daytime classification

The first nine PCs of the daytime dataset explained 76% of the total variance contained in the acoustic profiles at 38, 70 and 120 kHz (Figure 4a). These nine PCs were used to classify the acoustic profiles through hierarchical clustering (Figure 5b). The resulting classification was projected along the first two PCs (Figure 5c) and along geographical coordinates (Figure 5d,e).

Three acoustic seascape classes were found, one associated with slope-boundary waters in any of the two sampling periods (D1), and two in the Fernando de Noronha chain separated in time. One in Spring 2015 (D2) and one in Fall 2017 (D3). PCs 1 and 2—nearly representing 50% of the total seascape variance—show that the major differences between acoustic profiles were firstly found between 200 and 500 m depth (Figure 4f–h), and second, between 100 and 300 m depth (Figure 4i–k). Both modes of variance were consistent across frequencies. Profile variance was useful to identify the main differentiating features between seascape classes. For example, positive weights in PCs 1 and 2 show profiles with low backscatter at 300–500 m and high backscatter at 100–300 m depth (Figure 4f–k). In the PC space, we can see that these coordinates correspond to the acoustic seascape D1 (Figure 4c), associated with slope-boundary waters (Figure 4d,e). These differences were also evident in the classification of acoustic profiles. The acoustic seascape in slope-boundary waters (D1, Figure 4l–n) and near the Fernando de Noronha chain in Spring 2015 (D2, Figure 4o–q) were characterized by a weak mesopelagic backscatter signal in comparison to the Fernando de Noronha chain in Fall 2017 (D3, Figure 4r–t). The second important difference was the decay of signal between 100 and 300 m depth in the Fernando de Noronha chain in comparison to slope-boundary waters. As we can see in Figure 4o–q, this was specially marked in Spring 2015, suggesting a strong stratification between epipelagic and mesopelagic sound-scattering domains. Vertical integration values of acoustic backscatter and minor modes of daytime profile variance can be seen in supplementary material (Figures S2 and S3).

3.2 | Nighttime classification

The first nine PCs of the nighttime dataset explained 83% of the total variance contained in the acoustic profiles at 38, 70 and 120 kHz (Figure 4a). As in the daytime analysis, these nine PCs were used to classify the acoustic profiles through hierarchical clustering (Figure 4b), and the resulting classification was projected along the first two PCs (Figure 4c) and along geographical coordinates (Figure 4d,e).

Four major acoustic seascape classes were found, two associated with slope-boundary easterly waters in Spring 2015 (N1) and Fall 2017 (N2), and two associated with open-ocean westerly waters, also divided between Spring 2015 (N3) and Fall 2017 (N4). PCs 1 and 2—representing above 50% of the total seascape variance—show that the major differences between acoustic profiles were first concentrated between 200 and 500 m depth (Figure 5f–h) but also in a second mode of variance which evenly affected the acoustic profile all along the water column (Figure 5i–k). Modes of variance were overall consistent across frequencies. Looking at the PC weights along the acoustic profiles (Figure 5f–k) and at the classification results in the PC and geographical space (Figure 5c–e), we conclude that the first and second mode of variance operated in the spatial and temporal dimension, respectively. In other words, weak and strong mesopelagic backscatter divided slope-boundary

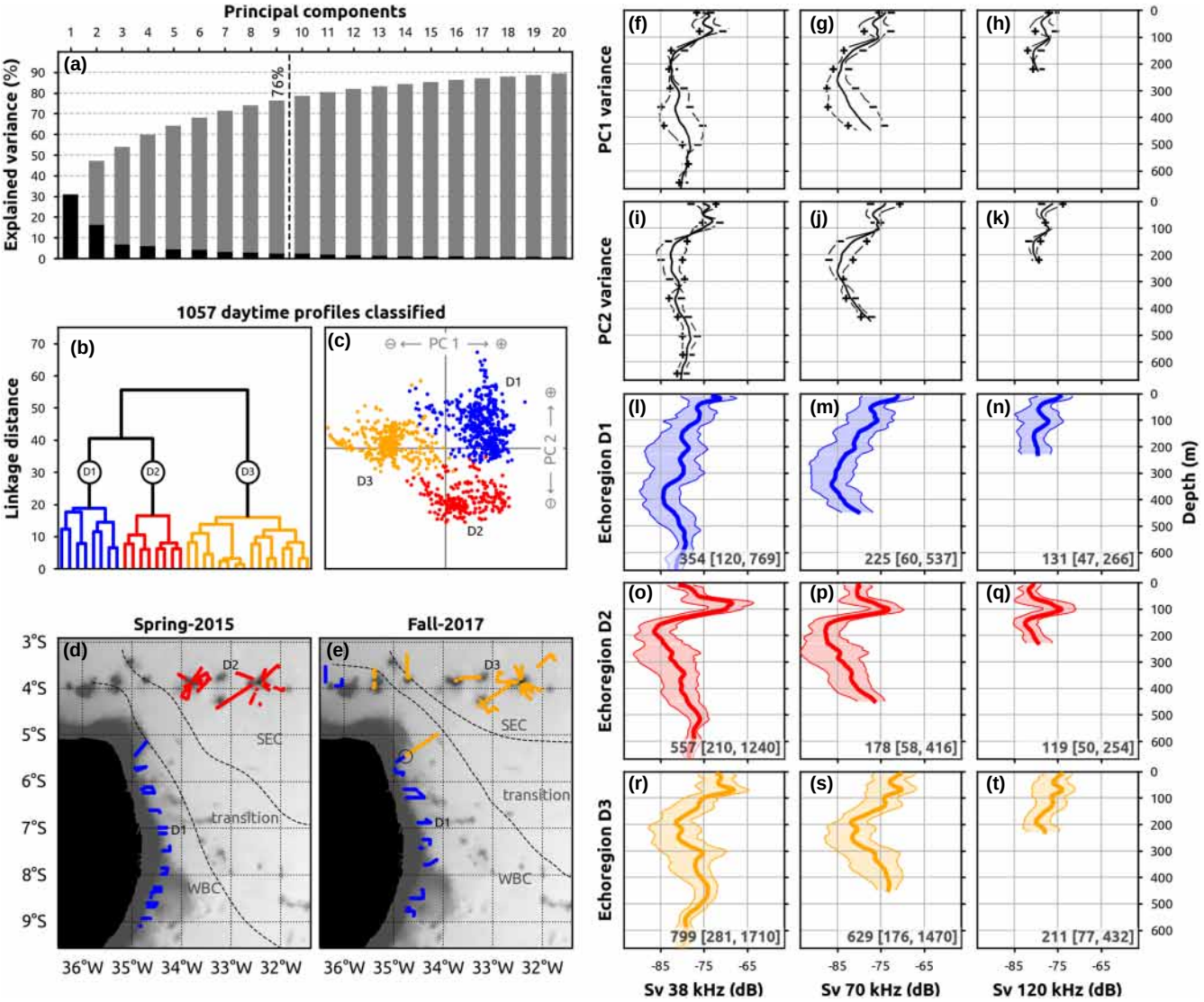

FIGURE 4 Variability and classification of daytime acoustic profiles. It shows the percentage of specific (black) and accumulated (grey) acoustic profile variance contained within each principal component (PC) (a), the clustering of profiles using the first nine PCs (b), and the classification of profiles projected along the first two PCs (c), and along geographical coordinates (d, e). It also shows the along-depth S_v variance contained within the first (f–h) and the second (i–k) PC, and three acoustic profile classes, associated with the echoregions D1 (l–n), D2 (o–q) and D3 (r–t). Acoustic profiles are shown at 38, 70 and 120 kHz. In variance profiles (f–k), central lines represent the mean, and lines with plus or minus symbols represent the variation over the mean after adding (+) or subtracting (–) each of the corresponding PC functions. In classification profiles (l–t), central lines represent the mean and side lines represent the 5%–95% percentile range. Numbers at the bottom indicate the vertically integrated backscatter of these lines, as the nautical area scattering coefficient (m^2 nmi^{-2}). Western-boundary and South-equatorial currents (WBC and SEC) are indicated according to Assunção et al. (2020).

westerly from open-ocean easterly waters, while weak and strong backscatter all along the water column changed from Spring 2015 to Fall 2017. These differences were also evident in the classification of acoustic profiles. Slope-boundary westerly waters in Spring 2015 (N1, Figure 5l–n) and Fall 2017 (N2, Figure 5o–q) were characterized by a weak mesopelagic backscatter in comparison to open-ocean easterly waters in Spring 2015 (N3, Figure 5r–t) and Fall 2017 (N4, Figure 5u–w). In agreement with the second mode of variance, these two regions presented similar acoustic profile shapes between sampling periods but with overall weaker backscatter in Spring 2015 and stronger in Fall 2017. Vertical integration values of acoustic backscatter and minor modes of nighttime profile variance can be seen in supplementary material (Figures S2 and S4).

4 | DISCUSSION

In this study, we apply a novel approach based on FDA to characterize the three-dimensional distribution of sound-scattering biota in oceanic waters off northeastern Brazil. By taking into account all the backscatter signal contained in multifrequency profiles, we successfully partitioned the seascape and defined spatially and temporally

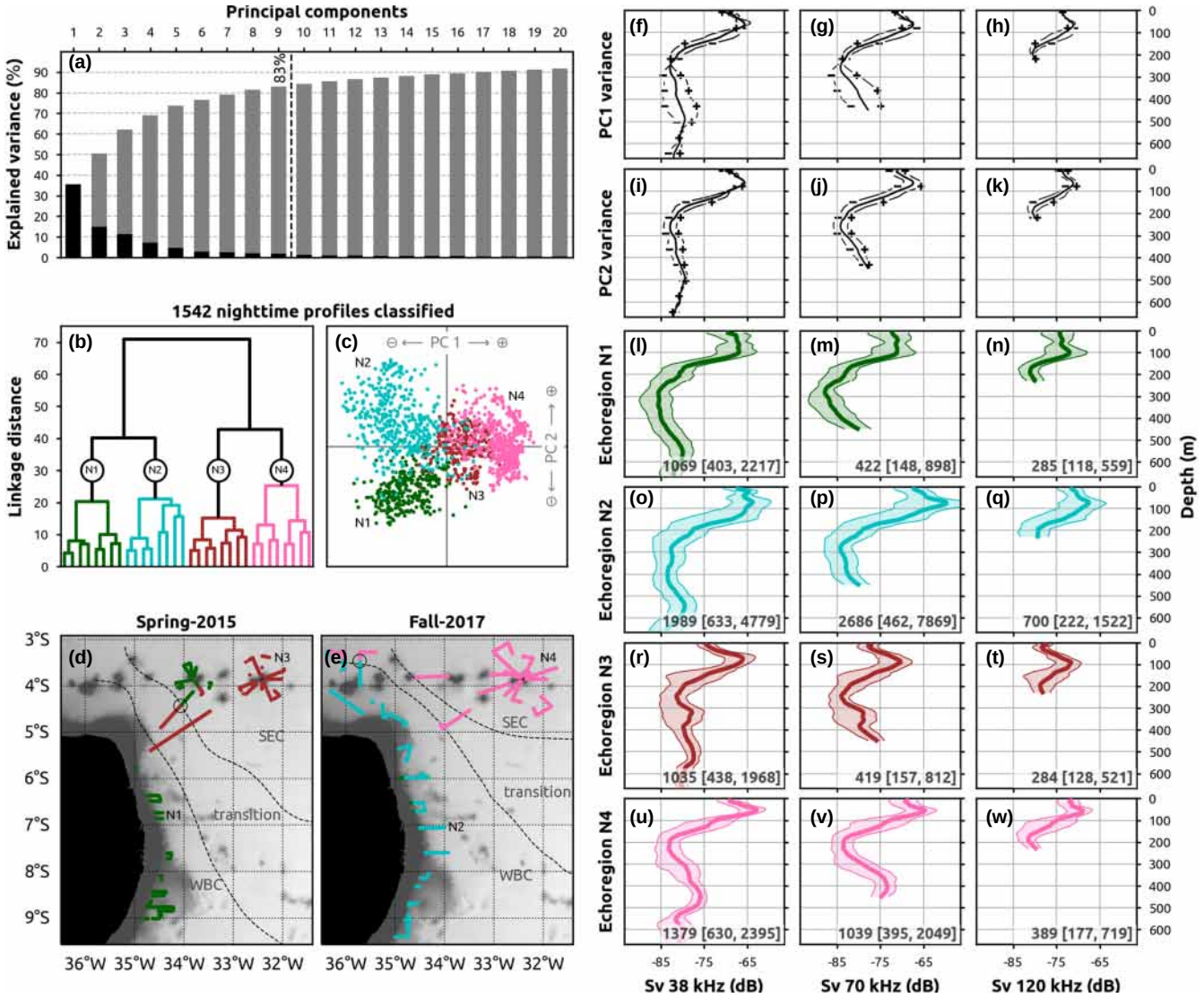

FIGURE 5 Variability and classification of nighttime acoustic profiles. It shows the percentage of specific (black) and accumulated (grey) acoustic profile variance contained within each principal components (PC) (a), the clustering of profiles using the first nine PCs (b), and the classification of profiles projected along the first two PCs (c), and along geographical coordinates (d, e). It also shows the along-depth S_v variance contained within the first (f–h) and the second (i–k) PC, and four acoustic profile classes, associated with the echoregions N1 (l–n), N2 (o–q), N3 (r–t) and N4 (u–w). Acoustic profiles are shown at 38, 70 and 120 kHz. In variance profiles (f–k), central lines represent the mean, and lines with plus or minus symbols represent the variation over the mean after adding (+) or subtracting (–) each of the corresponding PC functions. In classification profiles (l–w), central lines represent the mean and side lines represent the 5%–95% percentile range. Numbers at the bottom indicate the vertically integrated backscatter of these lines, as the nautical area scattering coefficient (m^2 nmi^{-2}). Western-boundary and South-equatorial currents (WBC and SEC) are indicated according to Assunção et al. (2020).

coherent echoregions with consistent acoustic features (Figures 4 and 5). We discuss below the application of FDA in acoustic data, the abiotic factors driving the seascape partitioning, and the ecological interpretation of this partitioning.

4.1 | Why functional acoustics?

Perhaps the most obvious advantage of FDA, compared to other statistical methods, is the ability to capture the distribution of variance along the physical continuum in which the signal is measured. This is of paramount importance when it comes to echosounder data, which is inherently functional, and registers the distribution of organisms along the depth dimension. In fact, one of the features that emerged as the most informative through the classification process in this study was the examination of backscattering variance along the depth dimension (see Figures 4f–k and 5f–k). This allowed to describe and diagnose the different modes of variation for any depth interval and frequency, facilitating the interpretation of similarities and dissimilarities between echoregions.

Another attractive aspect in the context of pelagic ecology is that FDA operates in a comprehensive way, capturing and analysing

all phenomena occurring within the acoustic profile. There is no need to select specific parts of the signal, such as layers or schools. This might be convenient when attempting to describe particular targets or aggregations (Coetzee, 2000; Proud et al., 2015), but it is limiting when studying the acoustic seascape as a whole. Certainly, peaks in acoustic profiles might represent layers or schools but these are not the only features considered. Signal drops are equally described in a basis function system because S_v thresholds are not applied during the process. Target detection algorithms also imply further computation in processing workflows, often adding reliability and scalability constraints in large-scale applications.

The smoothing process used to approximate basis functions to discrete data also constitutes the first step towards dimension reduction and was very convenient to bypass high-frequency variance and prioritize broader vertical patterns in the acoustic profiles (see Figure 3). This step can therefore be regarded as a vertical downsampling method itself but with some advantages in comparison to the average operations commonly used in acoustic data resampling. For instance, while results from averaging operations are not sensitive to the distribution of data within the resampling bins, function coefficients tell about the shape of data within known depth intervals, which are in addition affected by continuity constraints from adjacent data in the profile (Ramsay & Silverman, 2005). After fPCA and clustering, these coefficients can be used to reconstruct the acoustic profiles to the original resolution through the evaluation of basis functions. Functional smoothing provides therefore an elegant solution to reduce the vertical resolution of acoustic profiles while maximizing the retention of meaningful properties from the original data.

With a multifrequency approach, FDA also offers a convenient way to segment pelagic ecosystems based on the vertical distribution of distinct acoustic populations. Most seascape classification methods are based on single-frequency data, either designing metrics that describes the profiles features (Proud et al., 2015, 2018; Urmy et al., 2012) or using the profile signal itself as descriptors (Receveur et al., 2020). Recently, Lee and Staneva (2020) proposed an efficient method to extract temporal patterns from echosounder time series based on multifrequency data, demonstrating the utility of this approach to describe ecological processes for different biological components in the water column. Here, using multivariate FDA, we explicitly include depth-distribution analysis in combination with multifrequency analysis to describe pelagic ecosystems. This holistic approach can be especially useful in biogeographical studies, where the spatial variation in the numbers and types of organisms is key to determine the distribution of ecoregions (Longhurst, 2010; Spalding et al., 2007). As demonstrated in this study, multifrequency functional acoustics can efficiently describe the spatial variation in the numbers and types of features detected in the water column.

4.2 | Alternative implementations of the method

The present study provides a new application of FDA to classify acoustic seascapes using ship-borne multifrequency echosounder data. In particular, we propose a solution to analyse frequencies with variable depth range, we provide fully documented open-source code to implement the method (EchoPY v1.1, 2020), and we show with ancillary environmental and biological data that the classification obtained is consistent with other regionalization methods. However, decisions on the depth range and frequencies used will be survey specific, depending on frequency availability and signal-to-noise (weather) conditions. Decisions related to spatial resolution will depend on the objectives of the study. For instance, in the present work, we aimed at analysing regional-scale features, essentially sound-scattering layers which typically presented a vertical extent greater than 10 m. We found therefore appropriate to use a 10 m vertical resolution function system on profiles averaged every 2000 m in the horizontal (see methods Section 2.3.1 and Figure 3). Other case studies may target ephemeral horizontal features such as fish schools or thinner sound-scattering layers, with a different suite of frequencies and depth ranges. For that purpose, the open-source application associated with this study provides function arguments to tune these parameters conveniently (EchoPY v1.1, 2020).

4.3 | Physical to acoustical seascapes

By applying FDA on temperature and salinity profiles collected in parallel to the acoustic data presented here, Assunção et al. (2020) defined three different thermohaline areas: the western-boundary and south-equatorial current systems (WBC and SEC) and the transition area in between (see Figures 4d,c and 5d,c). In the present study, echoregions systematically distributed either in slope-boundary or open-ocean areas, matching these thermohaline systems. The only exception to this occurred in the nighttime Spring 2015 dataset, where the slope-boundary and the Rocas Atoll were classified together as the same echoregion, despite they were geographically separated by the WBC-SEC transition area (Figure 5d). This result, which may appear a contradiction, seems to illustrate particular physical processes taking place around the Rocas Atoll. This area is where the North Brazil Undercurrent (NBUC) coalesces on its way north with the westward central branch of the South Equatorial Current (cSEC; Dossa et al., 2021). The Rocas Atoll area is also where the eastward South Equatorial Undercurrent (SEUC) is originated. The generation of the SEUC is still a matter of debate, but it has been proposed to be intermittently fed by a retroflected branch of the NBUC reaching the area of the Rocas Atoll. Water masses features and float trajectories suggest this connection, at least in the spring season (Fischer et al., 2008; Johns et al., 1990). Furthermore, water masses with NBUC oxygen characteristics were found around the Rocas Atoll in Spring 2015, suggesting such NBUC-SEUC confluence (Costa da Silva et al., 2021). This is in agreement with our observations of similar acoustic seascapes between the slope-boundary area and the Rocas Atoll (Figure 5d). As this similarity is only found during nighttime, we believe that diel vertical migrants inhabiting subsurface waters from the NBUC are involved. Either they are out of

our sampling range during daytime or they are gas-bearing organisms, such as fish or siphonophores, that become distinguishable at night when they enter in resonance, due to pressure changes during ascent (Godø et al., 2009).

In addition to the coherent distribution between echoregions and physical provinces, acoustic seascape transitions coincided with bathymetric and oceanographic features registered in parallel to the acoustic survey. A fine look at these transitions provides further information about the processes in play (Figure 6). In one case, the transition occurred within the WBC system but in a region of strong bathymetric gradient (Figure 6a,b). In the other two cases, the echoregion limits were clearly related to abrupt changes in current velocity and direction (Figure 6c–f), which indicated the transition between the WBC and the SEC systems (Dossa et al., 2021). In all cases, multifrequency echograms showed vertical relocations and frequency-response changes in sound-scattering layers which, in turn, indicates a change in the vertical distribution and composition of sound-scattering fauna. These seascape snapshots near the echoregion fronts illustrate the high degree of fitness between hydrological and ecological transitions in the study area.

Echoregions also varied seasonally, in phase with the variability of the thermohaline structure (Assunção et al., 2020), currents (Dossa et al., 2021) and primary production (Farias et al., 2022). The slope-boundary area was characterized by a relatively stable thermohaline structure across seasons. In contrast, open-ocean waters of the Fernando de Noronha Chain exhibited a stronger seasonal modulation, with the mixed layer extending down to 92 m depth in Spring 2015, but hardly reaching 46 m depth in Fall 2017 (Assunção et al., 2020; Dossa et al., 2021). The seasonality was thus less marked in the slope-boundary area than in open-ocean waters. Accordingly, daytime acoustic seascape was classified in a unique echoregion in the slope-boundary but varied in the Fernando de Noronha Chain (Figure 4c,d). Particularly, in the Fernando de

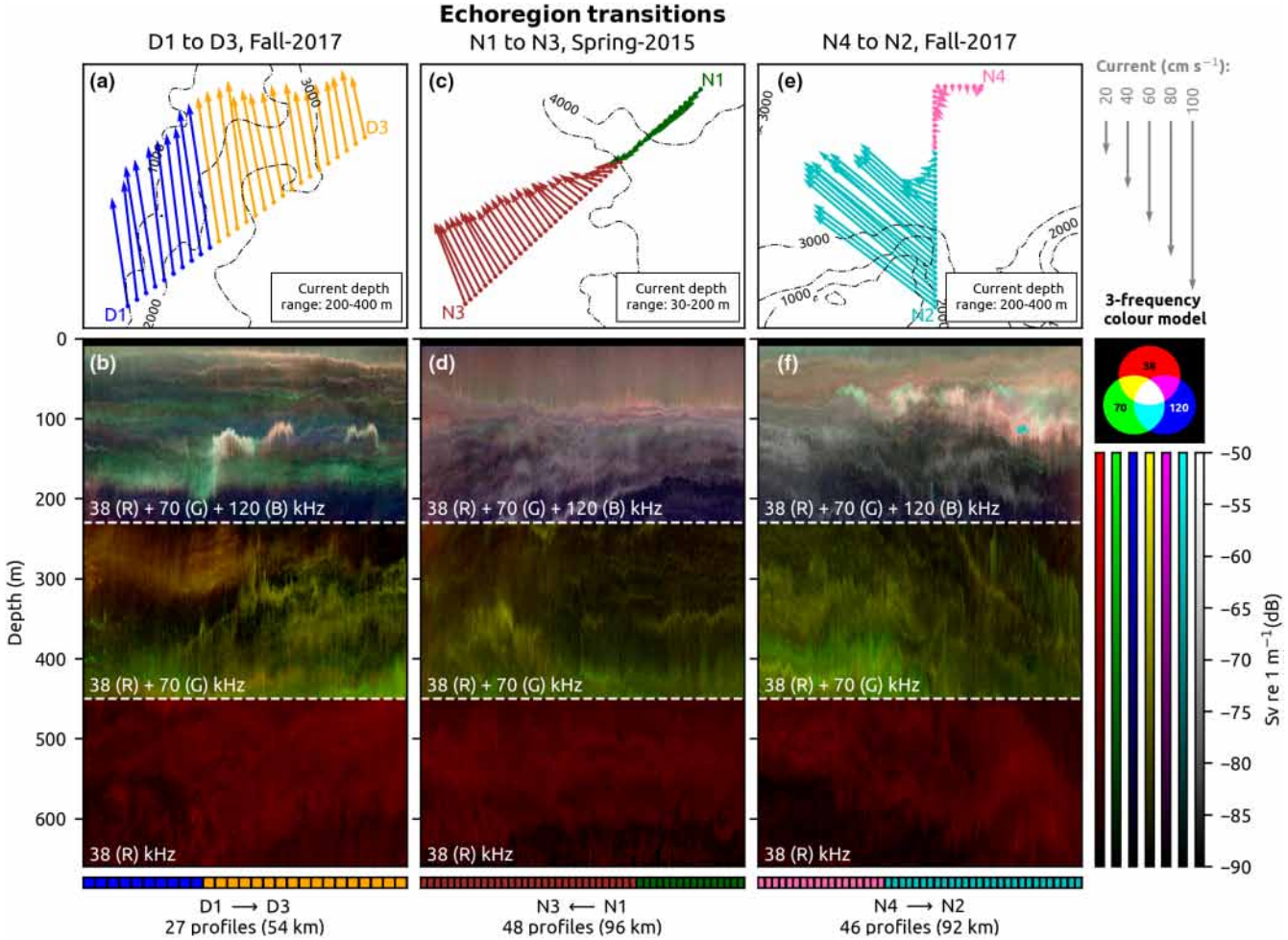

FIGURE 6 Examples of transitions between echoregions. Ship tracks are shown (top panels) with arrows indicating the mean current velocity and direction at particular depth ranges, colours indicating the echoregion to which each position belongs, and dashed lines indicating the isobaths. The location of these transitions are indicated with black circles in Figures 4e and 5d,e. Multifrequency echograms are displayed (bottom panels) using a RGB additive colour model in which red, green and blue indicate the contribution of backscatter (S_v) at 38, 70 and 120 kHz, respectively, and brightness indicate the average intensity of the three frequencies combined. Horizontal dashed lines in white indicate the number of frequencies involved at each depth range. A diagram is provided in the right side with hues for distinct combinations of frequencies and brightness scales. Alternatively, transitions are shown with single-frequency echograms in Figure S5.

Noronha Chain, acoustic backscattering in Spring 2015 experimented a sharp decline right below the base of the mixed layer, near 100 m depth (Figure 4o–q), when compared to profiles in the same area in Fall 2017 (Figure 4r–t). In addition to a sharp thermocline, a strong current shear was observed in this area in Spring 2015 between surface and subsurface waters, in contrast to Fall 2017 (Costa da Silva et al., 2021). These seasonal hydrographic changes were accompanied with primary production changes that were nicely mirrored by the acoustic seascape observed in the present study. In fact, increases in primary production in Fall 2017 (Farias et al., 2022) coincided with increases in water-column backscatter (see Figures 4 and 5), a proxy of secondary and tertiary biological production in the ocean (Irigoien et al., 2014). Horizontal and vertical physical processes are indeed known to shape the ecological seascape from primary production to top predators through bottom-up structuring (Bertrand et al., 2014). Our approach therefore proved efficient to decouple the physical features in place and to define consistent acoustic seascapes coherently distributed in space and time.

4.4 | Acoustic to biological seascapes

The term 'frequency response' or 'acoustic signature' refers to the along-frequency backscattering signal of acoustic targets, which has been historically exploited to identify single organisms or aggregations in the form of layers and shoals (Fernandes et al., 2005; Korneliussen et al., 2018). Here, the along-depth S_v signal at multiple frequencies has been used to partition acoustic seascapes, moving the multifrequency classification concept to the level of community. Indeed, what we termed here as 'echoregions' are areas with particular assemblages of distinct acoustic populations, as derived from the along-depth distribution and frequency response of targets. Echoregions are related with the concept of 'acoustic populations' introduced by Gerlotto (1987), where the distribution and properties of fish schools were gathered into geographical squares to classify and delineate pelagic communities. When describing echoregions, and similarly to other multifrequency methods, the major challenge is not only the classification, but also the identification of the features classified (Fernandes et al., 2005; Korneliussen et al., 2018). With echoregions the problem escalates, as we ought to describe multiple acoustic populations distributed along the water column.

Describing the species composition and assemblage within each echoregion is beyond the scope and falls outside the objectives of the present study. Vertically stratified trawling was not available to reveal the identity of particular acoustic aggregations. Yet, pelagic trawls and bongo nets deployed in Fall 2017 outlined species distribution patterns compatible with our observations with acoustic echosounders (Figure 7). *Pyrosoma atlanticum*, for instance, was exclusively found around the continental slope (Figure 7d; Tosetto et al., 2022) while psysonect siphonophores found in epipelagic waters were much more abundant around the Fernando de Noronha archipelago (Figure 7e). Eduardo et al. (2021) also identified in Fall 2017 different assemblages of mesopelagic lanternfish species, distributed between the west and east of the Fernando de Noronha chain (Figure 7f), mirroring our acoustic seascape regionalization. All these organisms are efficient sound reflectors at the frequencies used in the present study and they might be responsible of the acoustic seascape variance observed at epipelagic and mesopelagic depths (Figures 4f–k and 5f–k). For instance, preliminary results on the acoustic properties of pyrosomes suggest that they can form prominent sound-scattering layers at 38 kHz (Ohman, 2019). Likewise, psysonect siphonophores and mesopelagic fish species are among the most important groups contributing to sound scattering in the water column, due to the presence of resonant gas bladders in their bodies (Agersted et al., 2021; Proud et al., 2019). Combined, all these abundant sound-scattering animals—and likely others not captured by our sampling nets—contributed to the formation of the acoustic seascape in northeastern Brazil.

Based on the above we consider echoregions as biologically meaningful areas that help to delineate pelagic ecosystems in a cost-efficient and non-intrusive way. However, care must be taken when interpreting acoustic seascape classifications. In principle, frequency response describes the composition of the features identified within the acoustic seascape, while the distribution of these features tells about their vertical assemblage. However, this may not always be the case. For example, gas-bearing species are known to change their frequency response as they move vertically in the water column (Godø et al., 2009). Consequently, two acoustic features with distinct frequency response and depth distribution may eventually represent the same biological aggregation. In any case, differences between echoregions always imply either a change in the properties or in the vertical assemblage of species. Both things might happen at the same time and both provide ecologically meaningful information to delineate biogeographical fronts in the ocean.

Another important consideration is that the frequencies used to classify echoregions covered different depth ranges. This is an unavoidable limitation when dealing with multifrequency data but it is important to bear this mind. Echoregions will be much more influenced by the frequency-rich acoustic seascape in epipelagic waters in comparison to deeper waters.

Finally, daytime and nighttime regionalization might be regarded as different but complementary approaches to delineate pelagic ecosystems. As shown in our results, both regionalization identified echoregions separated between slope-boundary and open-ocean areas, and between spring and fall in the open-ocean area. Yet, nighttime profiles showed a more complex regionalization in comparison to daytime profiles, providing an extra division between the Rocas Atoll and Fernando de Noronha Archipelago, and between spring and fall in the slope-boundary area (see Figures 4 and 5). Differences were expected since both classifications are exploiting different set of species to describe echoregions. For example, new targets might enter the depth interval being analysed or even strong targets can mask the weak ones as a result of vertical relocations between day and night (Godø et al., 2009; Peña et al., 2020). Additionally, some of these targets

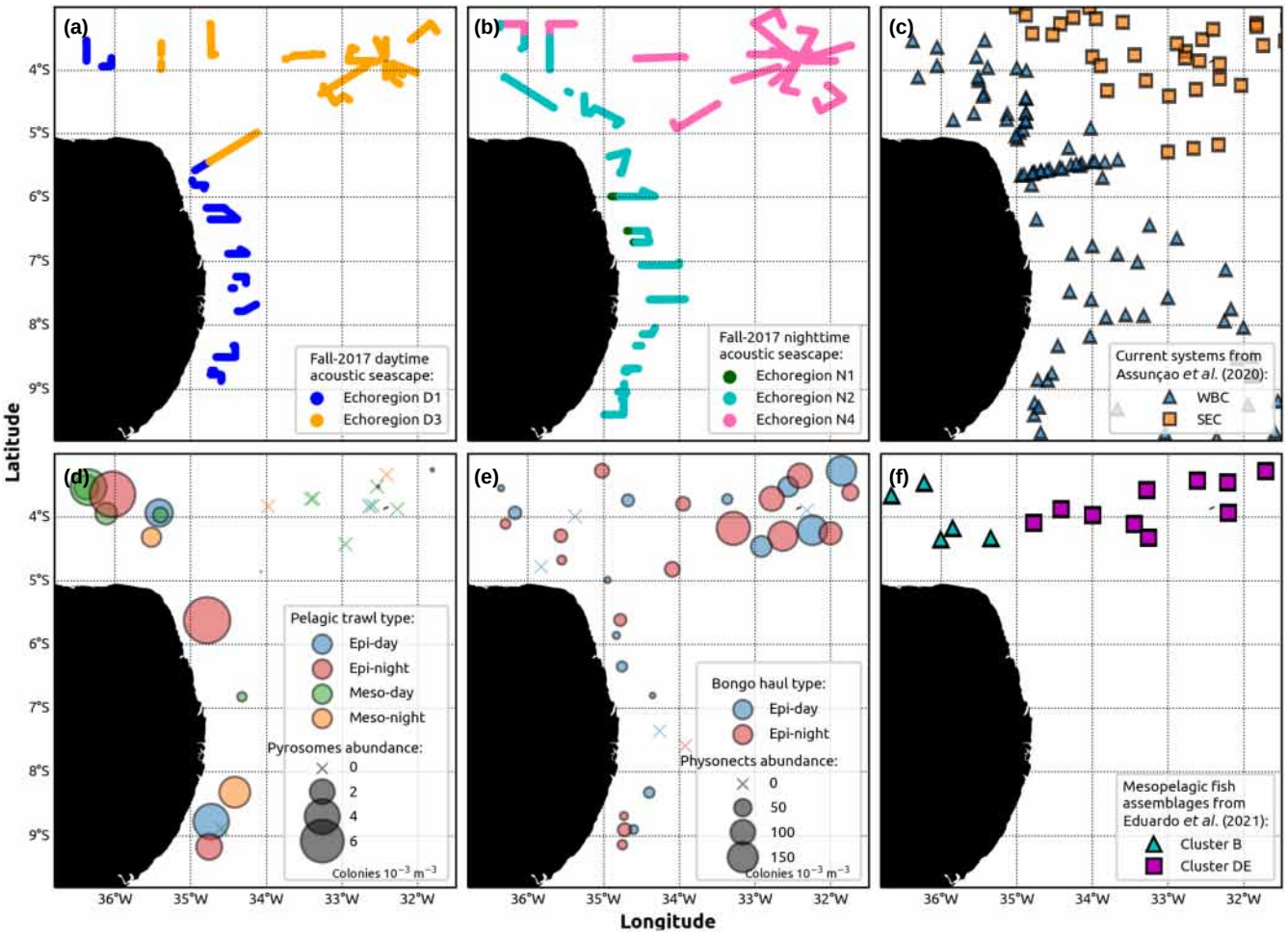

FIGURE 7 Day (a) and night (b) acoustic seascape regionalization compared to the distribution of current systems (c), pyrosomes (d), physonect siphonophores (e) and mesopelagic fish assemblages (f) in Fall 2017. Pyrosome and physonect abundances were analysed for the present study, circle colours indicate the sampling depth (epipelagic–mesopelagic) and time (day–night), circle size indicate abundance of colonies per $10^{-3} \cdot m^{-3}$. Current systems and mesopelagic fish assemblages come from Assunção et al. (2020) and Eduardo et al. (2021), respectively. See methods Section 2.5 for further details.

can be associated with different environmental thresholds and current systems. We advise therefore to interpret daytime and nighttime regionalization separately.

5 | CONCLUSION

Functional data analysis enabled to explicitly account for the shape of multifrequency acoustic profiles, and exploit this information to objectively describe and classify sound-scattering regions in the ocean. Similarly to biogeographical classifications, based on the spatial variation in the numbers and types of organisms in the ecosystem, this method simultaneously considers the vertical distribution, the intensity and the frequency response of the acoustic signal. Our regionalization differentiated slope-boundary and open-ocean systems and two contrasting hydrological regimes in spring and fall. Regions borders coincided with continental margins and current fronts, illustrating the match between biological and physical transitions in the ocean at the scale of kilometres, and suggesting a strong bottom-up structuring in the pelagic system off northeastern Brazil. The acoustic seascape consistency and the spatiotemporal coherence of the regions classified show that the method is efficient at identifying homogeneous and cohesive sound-scattering communities. Comparisons against hydrological and biological regionalization also show that the method is biogeographically consistent. Based on the term 'ecoregion', used in biogeography to areas with characteristic species assemblages, we propose the use of the term 'echoregion' when these communities have been identified through the examination of echosounder data, and they accomplish with the conditions of acoustic seascape consistency and spatiotemporal coherence. The method proposed here and the associated open-source application can be implemented to any acoustic dataset to define echoregions in the aquatic environment.

ACKNOWLEDGEMENTS

We acknowledge the French oceanographic fleet for funding ABRACOS I and ABRACOS II ship-time and the officers and crew of the R/V Antea for their contribution to the success of the operations

at sea. A.A. was funded by a post-doctoral IRD Fellowship. This work is a contribution to and was supported by the International Joint Laboratory TAPIOCA (www.tapioca.ird.fr), and the Horizon 2020 UE Projects PADDLE (grant agreement no. 73427) and TRIATLAS (grant agreement no. 817578). All collecting methods and specimen handling procedures were approved and carried out in accordance with relevant guidelines and regulations of the Brazilian Ministry of Environment (SISBIO; authorization number 47270-4 for ABRAÇOS 1 and 47270-5 for ABRAÇOS 2).

CONFLICT OF INTEREST

The authors declare no conflict of interests.

DATA AVAILABILITY STATEMENT

Environmental and acoustic data used in the present study are available in https://doi.org/10.17600/15005600 and https://doi.org/10.17600/17004100.

ORCID

Alejandro Ariza https://orcid.org/0000-0001-7864-4381
Everton Tosetto https://orcid.org/0000-0002-4020-0942

REFERENCES

Agersted, M. D., Khodabandeloo, B., Klevjer, T. A., García-Seoane, E., Strand, E., Underwood, M. J., & Melle, W. (2021). Mass estimates of individual gas-bearing mesopelagic fish from in situ wideband acoustic measurements ground-truthed by biological net sampling. *ICES Journal of Marine Science*, *78*, 3658–3673.

Aksnes, D. L., Røstad, A., Kaartvedt, S., Martinez, U., Duarte, C. M., & Irigoien, X. (2017). Light penetration structures the deep acoustic scattering layers in the global ocean. *Science Advances*, *3*(5), e1602468.

Ariza, A., Garijo, J., Landeira, J., Bordes, F., & Hernández-León, S. (2015). Migrant biomass and respiratory carbon flux by zooplankton and micronekton in the subtropical northeast Atlantic Ocean (Canary Islands). *Progress in Oceanography*, *134*, 330–342.

Assunção, R. V., Silva, A. C., Roy, A., Bourlès, B., Silva, C. H. S., Ternon, J.-F., Araujo, M., & Bertrand, A. (2020). 3D characterisation of the thermohaline structure in the southwestern tropical Atlantic derived from functional data analysis of in situ profiles. *Progress in Oceanography*, *187*, 102399.

Béhagle, N., Cotté, C., Ryan, T. E., Gauthier, O., Roudaut, G., Brehmer, P., Josse, E., & Cherel, Y. (2016). Acoustic micronektonic distribution is structured by macroscale oceanographic processes across 20–50 S latitudes in the South-Western Indian Ocean. *Deep Sea Research Part I: Oceanographic Research Papers*, *110*, 20–32.

Benoit-Bird, K. J., & Lawson, G. L. (2016). Ecological insights from pelagic habitats acquired using active acoustic techniques. *Annual Review of Marine Science*, *8*(1), 463–490.

Bertrand, A. (2015). *ABRACOS cruise*. RV Antea. https://doi.org/10.17600/15005600

Bertrand, A. (2017). *ABRACOS 2 cruise*. RV Antea. https://doi.org/10.17600/17004100

Bertrand, A., Chaigneau, A., Peraltilla, S., Ledesma, J., Graco, M., Monetti, F., & Chavez, F. P. (2011). Oxygen: A fundamental property regulating pelagic ecosystem structure in the coastal southeastern tropical Pacific. *PLoS One*, *6*(12), e29558.

Bertrand, A., Grados, D., Colas, F., Bertrand, S., Capet, X., Chaigneau, A., Vargas, G., Mousseigne, A., & Fablet, R. (2014). Broad impacts of fine-scale dynamics on seascape structure from zooplankton to seabirds. *Nature Communications*, *5*(1), 5239.

Boswell, K. M., D'Elia, M., Johnston, M. W., Mohan, J. A., Warren, J. D., Wells, R. J. D., & Sutton, T. T. (2020). Oceanographic structure and light levels drive patterns of sound scattering layers in a low-latitude oceanic system. *Frontiers in Marine Science*, *7*, 51.

Brodeur, R. D., Seki, M. P., Pakhomov, E. A., & Suntsov, A. V. (2005). Micronekton—What are they and why are they important? *Pices Press*, *13*, 7–11.

Choy, C., Wabnitz, C., Weijerman, M., Woodworth-Jefcoats, P., & Polovina, J. (2016). Finding the way to the top: How the composition of oceanic mid-trophic micronekton groups determines apex predator biomass in the central North Pacific. *Marine Ecology Progress Series*, *549*, 9–25.

Coetzee, J. (2000). Use of a shoal analysis and patch estimation system (SHAPES) to characterise sardine schools. *Aquatic Living Resources*, *13*(1), 1–10.

Costa da Silva, A., Chaigneau, A., Dossa, A., Eldin, G., Araujo, M., & Bertrand, A. (2021). Surface circulation and vertical structure of upper ocean variability around Fernando de Noronha archipelago and Rocas Atoll during spring 2015 and fall 2017. *Frontiers in Marine Science*, *8*, 598101.

de Boor, C. (1978). *A practical guide to splines* (Vol. *27*). Mathematics of Computation. Springer.

De Robertis, A., & Higginbottom, I. (2007). A post-processing technique to estimate the signal-to-noise ratio and remove echosounder background noise. *ICES Journal of Marine Science*, *64*(6), 1282–1291.

Demer, D. A., Berger, L., Bernasconi, M., Bethke, E., Boswell, K., Chu, D., Domokos, R., Dunford, A., Fassler, S., Gauthier, S., Hufnagle, L. T., Jech, J. M., Bouffant, N., Lebourges-Dhaussy, A., Lurton, X., Macaulay, G. J., Perrot, Y., Ryan, T., Parker-Stetter, S., … Williamson, N. (2015). *Calibration of acoustic instruments*. ICES Cooperative research report 326.

Dornan, T., Fielding, S., Saunders, R. A., & Genner, M. J. (2019). Swimbladder morphology masks Southern Ocean mesopelagic fish biomass. *Proceedings of the Royal Society B*, *286*, 20190353.

Dossa, A. N., Costa da Silva, A., Chaigneau, A., Eldin, G., Araujo, M., & Bertrand, A. (2021). Near-surface western boundary circulation off Northeast Brazil. *Progress in Oceanography*, *190*, 102475.

EchoPY v1.1. (2020). *Fisheries acoustic data processing in python*. https://pypi.org/project/echopy

Eduardo, L. N., Bertrand, A., Mincarone, M. M., Martins, J. R., Frédou, T., Assunção, R. V., Lima, R. S., Ménard, F., Le Loc'h, F., & Lucena-Frédou, F. (2021). Distribution, vertical migration, and trophic ecology of lanternfishes (Myctophidae) in the Southwestern Tropical Atlantic. *Progress in Oceanography*, *199*, 102695.

Escobar-Flores, P. C., O'Driscoll, R. L., Montgomery, J. C., Ladroit, Y., & Jendersie, S. (2020). Estimates of density of mesopelagic fish in the Southern Ocean derived from bulk acoustic data collected by ships of opportunity. *Polar Biology*, *43*(1), 43–61.

Farias, G. B., Molinero, J.-C., Carré, C., Bertrand, A., Bec, B., & de Castro Melo, P. A. (2022). Uncoupled changes in phytoplankton biomass and size structure in the western tropical Atlantic. *Journal of Marine Systems*, *227*, 103696.

Fernandes, P. G., Korneliussen, R. J., Lebourges-Dhaussy, A., Masse, J., & Iglesias, M. (2005). *The SIMFAMI project: Species identification methods from acoustic multi-frequency information*. European Union report (Q5RS-2001-02054).

Fischer, J., Hormann, V., Brandt, P., Schott, F. A., Rabe, B., & Funk, A. (2008). South equatorial undercurrent in the western to central tropical Atlantic. *Geophysical Research Letters*, *35*(21), L21601.

GEBCO. (2019). *A continuous terrain model of the global oceans and land*. British Oceanographic Data Centre, National Oceanography Centre, NERC.

Gerlotto, F. (1987). *The concept of acoustic populations: Its use for analysing the results of acoustic cruises*. International Symposium on Fisheries Acoustics.

Godø, O. R., Handegard, N. O., Browman, H. I., Macaulay, G. J., Kaartvedt, S., Giske, J., Ona, E., Huse, G., & Johnsen, E. (2014). Marine ecosystem acoustics (MEA): Quantifying processes in the sea at the spatio-temporal scales on which they occur. *ICES Journal of Marine Science*, *71*(8), 2357–2369.

Godø, O. R., Patel, R., & Pedersen, G. (2009). Diel migration and swimbladder resonance of small fish: Some implications for analyses of multifrequency echo data. *ICES Journal of Marine Science*, *66*(6), 1143–1148.

Godø, O. R., Samuelsen, A., Macaulay, G. J., Patel, R., Hjøllo, S. S., Horne, J., Kaartvedt, S., & Johannessen, J. A. (2012). Mesoscale eddies are oases for higher trophic marine life. *PLoS One*, *7*(1), e30161.

Handegard, N. O., du Buisson, L., Brehmer, P., Chalmers, S. J., De Robertis, A., Huse, G., Kloser, R., Macaulay, G., Maury, O., Ressler, P. H., Stenseth, N. C., & Godø, O. R. (2013). Towards an acoustic-based coupled observation and modelling system for monitoring and predicting ecosystem dynamics of the open ocean. *Fish and Fisheries*, *14*(4), 605–615.

Irigoien, X., Klevjer, T. A., Røstad, A., Martinez, U., Boyra, G., Acuña, J. L., Bode, A., Echevarria, F., Gonzalez-Gordillo, J. I., Hernandez-Leon, S., Agusti, S., Aksnes, D. L., Duarte, C. M., & Kaartvedt, S. (2014). Large mesopelagic fishes biomass and trophic efficiency in the open ocean. *Nature Communications*, *5*(1), 3271.

Johns, W. E., Lee, T. N., Schott, F. A., Zantopp, R. J., & Evans, R. H. (1990). The North Brazil current retroflection: Seasonal structure and eddy variability. *Journal of Geophysical Research*, *95*, 22.

Kaartvedt, S., Klevjer, T., & Aksnes, D. (2012). Internal wave-mediated shading causes frequent vertical migrations in fishes. *Marine Ecology Progress Series*, *452*, 1–10.

Klevjer, T. A., Irigoien, X., Røstad, A., Fraile-Nuez, E., Benítez-Barrios, V. M., & Kaartvedt, S. (2016). Large scale patterns in vertical distribution and behaviour of mesopelagic scattering layers. *Scientific Reports*, *6*(1), 19873.

Korneliussen, R. J., Berger, L., Campanlla, F., Chu, D., Demer, D., De Robertis, A., Domokos, R., Doray, M., Fielding, S., Fässler, S. M. M., Gauthier, S., Gastauer, S., Horne, J., Hutton, B., Iriarte, F., Jech, J. M., Kloser, R., Lawson, G., Lebourges-Dhaussy, A., … Thompson, C. (2018). *Acoustic target classification*. ICES Cooperative research report, 344.

Lee, W.-J., & Staneva, V. (2020). Compact representation of temporal processes in echosounder time series via matrix decomposition. *The Journal of the Acoustical Society of America*, *148*(6), 3429–3442.

Longhurst, A. (2010). *Ecological geography of the sea*. Elsevier.

MacLennan, D., Fernandes, P. G., & Dalen, J. (2002). A consistent approach to definitions and symbols in fisheries acoustics. *ICES Journal of Marine Science*, *59*(2), 365–369.

Murray, J., & Hjort, J. (1912). *The depths of the ocean*. Macmillan and Co. Limited.

Nerini, D., Monestiez, P., & Manté, C. (2010). Cokriging for spatial functional data. *Journal of Multivariate Analysis*, *101*(2), 409–418.

Nero, R. W., Magnuson, J. J., Brandt, S. B., Stanton, T. K., & Jech, J. M. (1990). Finescale biological patchiness of 70 kHz acoustic scattering at the edge of the Gulf Stream—EchoFront 85. *Deep Sea Research Part A. Oceanographic Research Papers*, *37*(6), 999–1016.

Ohman, M. D. (2019). *California current ecosystem LTER program, CCE-P1908 cruise*. Cruise report.

Pauthenet, E., Roquet, F., Madec, G., & Nerini, D. (2017). A linear decomposition of the southern ocean thermohaline structure. *Journal of Physical Oceanography*, *47*(1), 29–47.

Peña, M., Cabrera-Gámez, J., & Domínguez-Brito, A. C. (2020). Multifrequency and light-avoiding characteristics of deep acoustic layers in the North Atlantic. *Marine Environmental Research*, *154*, 104842.

Proud, R., Cox, M., Le Guen, C., & Brierley, A. (2018). Fine-scale depth structure of pelagic communities throughout the global ocean based on acoustic sound scattering layers. *Marine Ecology Progress Series*, *598*, 35–48.

Proud, R., Cox, M. J., Wotherspoon, S., & Brierley, A. S. (2015). A method for identifying sound scattering layers and extracting key characteristics. *Methods in Ecology and Evolution*, *6*(10), 1190–1198.

Proud, R., Handegard, N. O., Kloser, R. J., Cox, M. J., & Brierley, A. S. (2019). From siphonophores to deep scattering layers: Uncertainty ranges for the estimation of global mesopelagic fish biomass. *ICES Journal of Marine Science*, *76*(3), 718–733.

Ramsay, J. O., & Silverman, B. W. (2005). *Functional data analysis*. Springer Series in Statistics.

Receveur, A., Menkes, C., Allain, V., Lebourges-Dhaussy, A., Nerini, D., Mangeas, M., & Ménard, F. (2020). Seasonal and spatial variability in the vertical distribution of pelagic forage fauna in the Southwest Pacific. *Deep Sea Research Part II: Topical Studies in Oceanography*, *175*, 104655.

Ryan, T. E., Downie, R. A., Kloser, R. J., & Keith, G. (2015). Reducing bias due to noise and attenuation in open-ocean echo integration data. *ICES Journal of Marine Science*, *72*(8), 2482–2493.

Saba, G. K., Burd, A. B., Dunne, J. P., Hernández-León, S., Martin, A. H., Rose, K. A., Salisbury, J., Steinberg, D. K., Trueman, C. N., Wilson, R. W., & Wilson, S. E. (2021). Toward a better understanding of fish-based contribution to ocean carbon flux. *Limnology and Oceanography*, *66*(5), 1639–1664.

Spalding, M. D., Fox, H. E., Allen, G. R., Davidson, N., Ferdaña, Z. A., Finlayson, M., Halpern, B. S., Jorge, M. A., Lombana, A., Lourie, S. A., Martin, K. D., McManus, E., Molnar, J., Recchia, C. A., & Robertson, J. (2007). Marine ecoregions of the world: A bioregionalization of coastal and shelf areas. *Bioscience*, *57*(7), 573–583.

Tosetto, E. G., Barkokébas Silva, B., Franchesca GarcÃa DÃaz, X., Neumann-LeitÃ£o, S., & Bertrand, A. (2022). Thaliacean community responses to distinct thermohaline and circulation patterns in the Western Tropical South Atlantic Ocean. *Hydrobiologia*.

Tosetto, E. G., Bertrand, A., Neumann-Leitão, S., Costa da Silva, A., & Nogueira Júnior, M. (2021). Spatial patterns in planktonic cnidarian distribution in the western boundary current system of the tropical South Atlantic Ocean. *Journal of Plankton Research*, *43*(2), 270–287.

Urmy, S. S., Horne, J. K., & Barbee, D. H. (2012). Measuring the vertical distributional variability of pelagic fauna in Monterey Bay. *ICES Journal of Marine Science*, *69*(2), 184–196.

BIOSKETCH

Alejandro Ariza is a post-doctoral researcher at the Institut de Recherche et Développement in Sète, France. He works on pelagic ecology in open-ocean systems. He combines net sampling and acoustic echosounders to understand the distribution and dynamics of zooplankton and micronekton in a changing ocean.

Author Contributions: Alejandro Ariza, Arnaud Bertrand, and Anne Lebourges-Dhaussy designed and coordinated the study. David Nerini and Etienne Pauthenet supervised the implementation of functional data analysis. Ramilla Assunção and Everton Tosetto contributed in the validation of the method with environmental and biological regionalization. Gildas Roudaut participated in acoustic data acquisition and processing. Alejandro

Ariza analysed the data and wrote the manuscript with contribution from all authors.

SUPPORTING INFORMATION

Additional supporting information can be found online in the Supporting Information section at the end of this article.

How to cite this article: Ariza, A., Lebourges-Dhaussy, A., Nerini, D., Pauthenet, E., Roudaut, G., Assunção, R., Tosetto, E., & Bertrand, A. (2022). Acoustic seascape partitioning through functional data analysis. *Journal of Biogeography*, *00*, 1–15. https://doi.org/10.1111/jbi.14534